Applied Microbiology and Biotechnology (2024) 108:483
https://doi.org/10.1007/s00253-024-13299-9

BIOTECHNOLOGICAL PRODUCTS AND PROCESS ENGINEERING

Identifying sesterterpenoids via feature-based molecular networking and small-scale fermentation

Kangjie Lv[1] · Yuyang Duan[1] · Xiaoying Li[1] · Xinye Wang[1] · Cuiping Xing[1] · Keying Lan[1] · Bin Zhu[2] · Guoliang Zhu[1] · Yuyang Qiu[3] · Songwei Li[4] · Tom Hsiang[5] · Lixin Zhang[1] · Lan Jiang[6] · Xueting Liu[1,6]

Received: 27 May 2024 / Revised: 12 August 2024 / Accepted: 30 August 2024 / Published online: 8 October 2024

Abstract

Terpenoids are known for their diverse structures and broad bioactivities with significant potential in pharmaceutical applications. However, natural products with low yields are usually ignored in traditional chemical analysis. Feature-based molecular networking (FBMN) was developed recently to cluster compounds with similar skeletons, which can highlight trace amounts of unknown compounds. Fusoxypene A is a sesterterpene synthesized by *Fusarium oxysporum* fusoxypene synthase (FoFS) with a unique 5/6/7/3/5 ring system. In this study, the FoFS-containing biosynthetic gene cluster was identified from *F. oxysporum* FO14005, and an efficient FBMN-based strategy was established to characterize four new sesterterpenoids, fusoxyordienoid A–D (**1**–**4**), based on a small-scale fermentation strategy. A cytochrome P450 monooxygenase, FusB, was found to be involved in the functionalization of fusoxypene A at C-17 and C-24 and responsible for the hydroxylation of fusoxyordienoid A at C-1 and C-8. This study highlights the potential of FBMN as a powerful tool for the discovery and characterization of natural compounds with low abundance.

Key points

- *Combined small-scale fermentation and FBMN for rapid discovery of fusoxyordienoids*
- *Characterization of four new fusoxyordienoids with 5/6/7/3/5 ring system*
- *Biosynthetic pathway elucidation via tandem expression and substrate feeding*

Keywords Bifunctional terpene synthases · Feature-based molecular networking · Cytochrome P450 · *Aspergillus oryzae* · Heterologous expression

Introduction

Terpenoids represent the largest family of natural products, characterized by their diverse structures and a broad range of bioactivities. Fungal bifunctional terpene synthase (BFTS) exhibits the potential to synthesize di- and sesterterpenes with unique and distinct structures (Toyomasu et al. 2007; Minami et al. 2018; Mitsuhashi and Abe 2018; Guo et al. 2021; Jiang et al. 2021a, 2022a, 2022b). Furthermore, tailoring genes within the gene clusters may introduce multiple functional groups on the terpenoid skeleton and lead to the production of a variety of novel compounds (Keller 2019).

Kangjie Lv and Yuyang Duan contributed equally to this work.

✉ Lan Jiang
jianglan0426@163.com

✉ Xueting Liu
liuxueting@ecust.edu.cn

[1] State Key Laboratory of Bioreactor Engineering, East China University of Science of Technology, Shanghai 200237, China

[2] Lab of Pharmaceutical Crystal Engineering Research and Technology, East China University of Science and Technology, Shanghai 200237, China

[3] School of Insurance, Shandong University of Finance and Economics, Jinan 250014, China

[4] School of Medicine, Shanghai University, Shanghai 200444, China

[5] School of Environmental Sciences, University of Guelph, 50 Stone Road East, Guelph, ON N1G 2W1, Canada

[6] Department of Cardiothoracic Surgery, Children's Hospital of Nanjing Medical University, Nanjing 210093, China

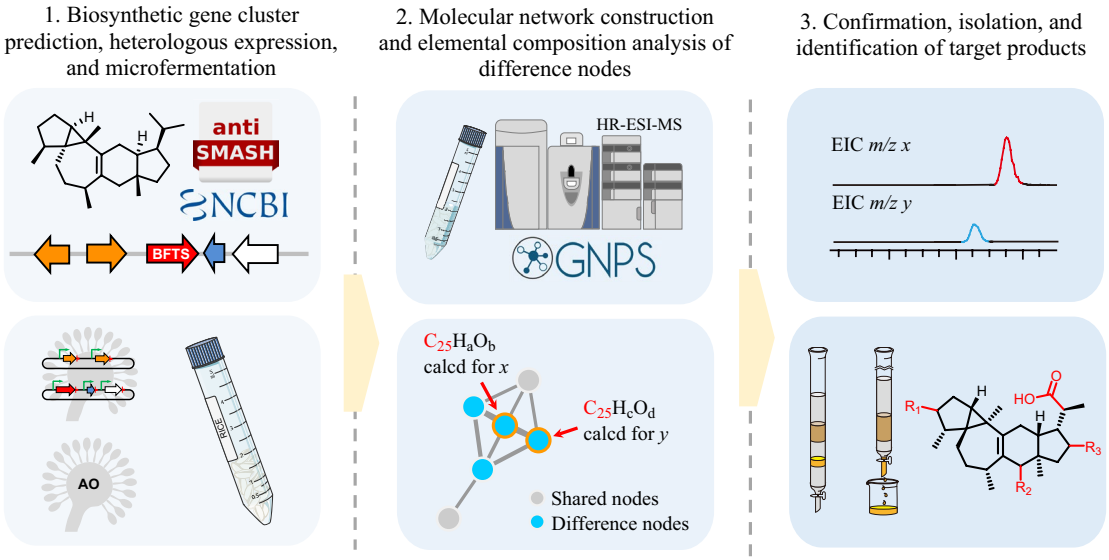

Scheme 1 Diagrammatic workflow for FBMN-assisted novel sesterterpenoids discovery

For example, ophiobolin F is transformed into ophiobolin A, a sesterterpenoid with anti-cancer activity, by P450 $OblB_{Ac}$ (Chiba et al. 2013; Narita et al. 2016). Similarly, the involvement of the P450 enzyme VndE in the degradation of variediene leads to the generation of a series of remarkable norditerpenoids featuring a 5/5 bicyclic ring system (Jiang et al. 2022a).

The development of chromatographic and spectroscopic techniques has increased the speed of natural product discovery, compelling researchers to seek out innovative compounds from low-yielding secondary metabolites (Pye et al. 2017; Zhang and Hong 2020; Gong et al. 2021), and a strategy for rapid and accurate detection of these trace products from crude extracts is required. Molecular networking (MN), which is commonly used for visualizing and annotating no-target mass spectrometry (MS) data, has been used to address this challenge (Watrous et al. 2012; Wang et al. 2016; Zhu et al. 2020; Han et al. 2022). And feature-based molecular networking (FBMN) (Nothias et al. 2020), a method that incorporates MS^1 information such as retention time into classical MN, could further distinguish isomers within the network (Afoullouss et al. 2022). With the combination of liquid chromatography, high-resolution mass spectrometry (LC-HRMS), and small-scale fermentation, target products could be determined quickly.

Previously, we demonstrated that FoFS, a BFTS identified from *Fusarium oxysporum* FO14005, is responsible for the biosynthesis of fusoxypene A (**5**), a sesterterpene with a unique 5/6/7/3/5 ring system (Jiang et al. 2021a). In this study, we identified the gene cluster in *F. oxysporum* FO14005 containing FoFS and adjacent cytochrome P450 monooxygenase, named it *fus*, and then heterologously transferred it into the target host *Aspergillus oryzae* (AO). A strategy combining small-scale fermentation (using 1 g rice medium) with FBMN was established (Scheme 1) for identifying four new sesterterpenoids, named fusoxyordienoids A–D (**1**–**4**), from AO-*orfADE*/*fusBC*. Further gene functional verification experiments showed that endogenous enzymes in AO and the P450 enzyme FusB in *fus* gene cluster jointly catalyzed the formation of fusoxyordienoids. We herein provide an efficient strategy for the rapid identification of trace amounts of specific natural products in small amounts of crude extract.

Materials and methods

General experimental procedures

The instruments, consumables, and reagents used in this experiment have been described in our previous report (Jiang et al. 2022a). Pyridine-d_5 (99.8 atom% enriched, Kanto) was used as the recording solvent to acquire NMR spectra. Chemical shifts of ^{1}H NMR were reported as δ value with pyridine (8.74, 7.58, and 7.22 ppm) as references. Chemical shifts of ^{13}C NMR were reported as δ value with pyridine (149.0, 135.3, and 123.3 ppm) as references. Unless stated otherwise, media, chemicals, and biological reagents were purchased from standard commercial sources.

Strains and media

F. oxysporum FO14005 was originally isolated from tomato in Guangdong, China. It was stored at − 20 °C

on wheat seed, subcultured onto 2% potato dextrose agar (PDA, Fisher Scientific), and incubated at 25 °C for 5 days, prior to cloning the BFTS and related tailoring genes. Strain *F. oxysporum* FO14005 has been deposited at the China General Microbiological Culture Collection Center (accession No. 21067).

The gene cluster was expressed in *A. oryzae* NSAR1 (*niaD*$^{-}$ *sC*$^{-}$ *adeA*$^{-}$ Δ*argB*::*adeA*$^{-}$) (Jin et al. 2004). For the growth of *A. oryzae* transformant strains, shake cultures were maintained at 30 °C and 220 rpm for 5 days in DPY medium (containing 1% polypeptone, 2% dextrin, 0.5% yeast extract, 0.01% $(NH_4)_2SO_4$, 0.01% adenine, 0.06% arginine, 0.15% methionine). *Escherichia coli* DH10b was utilized for cloning. A rice medium was used for the fermentation of *A. oryzae* transformant strains (80 g of rice added to a high-temperature-resistant polypropylene bag, with 120 mL of deionized water added).

Genomic DNA preparation

The genomic DNA of all these fungi used in this study was extracted following the procedure described in the literature. Mycelia collected from potato dextrose broth (PDB) were lyophilized in FreeZone Freeze Dry Systems (LABCONCO Corp., USA) overnight and ground with particles in 1.5-mL microcentrifuge tubes (SOURCE). Ground mycelium was resuspended with 700 µL of LETS buffer (pH 8.0, 10 mM Tris–HCl, 0.5% SDS, 0.1 M LiCl, 20 mM EDTA), followed by two rounds of extraction with phenol–chloroform-isoamyl alcohol (25:24:1). After extraction, the genomic DNA was precipitated from the supernatant by adding 2 volumes of ethanol. And the DNA was then washed with 70% ethanol, air dried, and then dissolved in sterile water. Finally, the genomic DNA was stored at − 20 °C until further experiments were conducted.

Preparation of expression plasmids

Five genes encoding *orfA*, *fusB*, *fusC*, *orfD*, and *orfE* gene sequences were amplified from *F. oxysporum* FO14005 genomic DNA using Q5® High-Fidelity DNA Polymerase (New England Biolabs, USA) with primer pairs shown in Table S1. To construct expression plasmids, each PCR product was inserted into vector pUARA4 or pUSA4 at the appropriate restriction site using ClonExpress®II One Step Cloning Kit (Vazyme Biotech, CN). All plasmids used in this experiment are listed in Table S2. The gene cluster sequences of the five genes have been deposited in the National Center for Biotechnology Information (NCBI) under accession number PP747339.

Transformation of A. oryzae

To construct transformant AO-*orfADE*/*fusBC* (pUSA4-*orfA*/*fusB* and pUARA4-*fusC*/*orfDE*), the protoplast of *A. oryzae* NSAR1 was prepared using the protoplast-polyethylene glycol method as described in a previous study (Oikawa 2020). In this context, AO refers to *A. oryzae*, and AO-*orfADE*/*fusBC* denotes a transformant of *A. oryzae* carrying *orfA*, *fusB*, *fusC*, *orfD*, and *orfE* genes. The AO transformants listed in Table S2 were cultivated on an MPY medium following a previously described method (Jiang et al. 2022a).

FBMN-based analysis for mining fusoxyordienoids

The AO-*orfADE*/*fusBC* was inoculated into a rice medium (1 g) and incubated at 30 °C for 5 days. Fermentation samples were thoroughly extracted with ethyl acetate (EtOAc) and subsequently concentrated under a vacuum. The dried EtOAc layer (1.7 mg) was analyzed using a Shimadzu LC-20AD UPLC coupled with a Thermo Scientific Q Exactive Obitrap mass spectrometer featuring an electrospray ionization (ESI) source in negative polarity. A Waters ACQUITY BEH C18 column (2.1 × 100 mm, 1.7 µm particles) was used for the UPLC analysis, and an acidic water/ACN gradient was applied as the mobile phase. An optimized data-dependent acquisition mode was used to analyze the 50 µg/mL methanol (MeOH) solution of the AO-*orfADE*/*fusBC* extract. The analytical procedure consisted of a full MS survey scan with a resolution of 70,000 in the mass range of 100–1200 Da (scan time was set at 50 ms), followed by an MS/MS scan of the ten most intense ions in the higher-energy collisional dissociation (HCD) trap at a resolution of 17,500. A collision energy of 40 eV was used for the MS/MS scan.

MSConvert software was used to convert raw mass data (Chambers et al. 2012). MZmine 2 software was used to screen ion peaks with MS^1 responsivity over $3.0E^6$ and MS^2 responsivity over $3.0E^3$ (Pluskal et al. 2010). The converted raw data of AO and AO-*orfADE*/*fusBC* and their feature data were submitted to the GNPS together, and the FBMN was analyzed with Min Pairs Cos at 0.75. There were 356 nodes in the range of *m/z* 300 − 500 selected for further analysis (Wang et al. 2016). This limited *m/z* range was postulated from the molecular weight of the intermediate fusoxypene A (**5**) with an introduction of an extra 1 − 5 oxygen atoms by the predicted tailoring enzymes.

Isolation process for fusoxyordienoids A–D (*1–4*)

The fermentation products of transformant AO-*orfADE*/*fusBC* were thoroughly extracted with EtOAc and concentrated under vacuum. The crude extract was then redissolved

with MeOH and extracted with dichloromethane (CH_2Cl_2) three times.

The CH_2Cl_2 layer underwent fractionation on a silica gel column using a mobile phase gradient CH_2Cl_2-MeOH (0 – 100%). This process resulted in the separation of the crude extract into ten sub-fractions (G1 – G10). LC–MS analysis of these fractions revealed some potential novel analogs of fusoxyordienoids in G1 – G4 and G5 – G7 based on the characteristic UV absorption and HRMS. The sub-fraction G1 – G4 (marked as G385) was further fractionated by a C18-RP silica gel using a gradient MeOH-H_2O (0 – 100%) as mobile phase to give nine sub-fractions (G385-F1 – F9). G385-F7 was further separated by Sephadex LH-20 eluting with MeOH to yield 35 sub-fractions (G385-F7-N1 – N35). LC–MS analysis of these fractions revealed some potential novel analogs of fusoxyordienoids in G385-F7-N6 – N10 based on the characteristic UV absorption and HRMS. After drying in vacuo, G385-F7-N6 – N10 (marked as G385-F7-N6N10) was subjected to further separation using a silica solid-phase extraction (SPE) column with a gradient mobile phase of petroleum ether (PE) and EtOAc (0 – 100%). This process yielded eight sub-fractions (G385-F7-N6N10-S1 – S8). LC–MS analysis of these fractions revealed that **1** and **4** were present in G385-F7-N6N10-S6 – S9. The sub-fraction G5 – G7 (marked as G401) was further fractionated by a C18-RP silica gel using a gradient MeOH-H_2O (0 – 100%) as mobile phase to give six sub-fractions (G401-F1 – F6). G401-F5 was further separated by Sephadex LH-20 elution with MeOH to yield 41 sub-fractions (G401-F5-N1 – N41). LC–MS analysis of these fractions revealed **2** and **3** in G401-F5-N5 – N9 based on the characteristic UV absorption and HRMS. The weights of the main fractions in the separation process are summarized in Table S3.

To isolate the target compound, G385-F7-N6N10-S6 – S9 was purified using semipreparative reversed-phase high-performance liquid chromatography (RP-HPLC) with an ACE C18-PFP (10 × 250 mm) column. The purification was achieved by eluting at a flow rate of 4.0 mL/min with an isocratic elution of 55% acetonitrile (ACN)-water, resulting in the isolation of **4** (0.2 mg, t_R = 7 min) and **1** (1.5 mg, t_R = 12 min). G401-F5-N5 – N9 (marked as G401-F5-N5N9) was purified by semipreparative RP-HPLC with an ACE C18-PFP (10 × 250 mm) column eluting at a flow rate of 4.0 mL/min using an isocratic elution (38% ACN-H_2O) to yield **3** (1.5 mg, t_R = 14.3 min) and **2** (4.0 mg, t_R = 14.9 min).

Biotransformation experiments

The biotransformation assay that used **1** as substrate was described previously (Jiang et al. 2022a). To feed **5**, AO and AO-*fusB* transformants were cultured for 1 day at 30 °C on MPY agar medium amended with appropriate nutrients. Compound **5** was dissolved at a concentration of 10 mg/mL in DMSO and then layered on the surface of the non-amended MPY medium, AO culture plates, and AO-*fusB* culture plates, respectively. Both the control sample and experimental sample were then incubated at 30 °C for 4 days, after which they were subjected to extraction with EtOAc. The organic phase was dried, dissolved in MeOH, and directly analyzed using LC-HRMS.

Biological assay

Antifungal bioassays were conducted using methods of the Clinical and Laboratory Standards Institute (CLSI) M-27A (Standards 1997). For antibacterial bioassays, the two-fold broth microdilution method outlined by the CLSI for antimicrobial susceptibility testing was used (Ro et al. 2006). The cytotoxicity of compounds **1** and **4** was evaluated using the CCK-8 method (Tominaga et al. 1999; Liu et al. 2011).

Results

Bioinformatic analysis of the fus gene cluster

Functional annotation of the genomic DNA where FoFS was located using the 2ndFind platform (http://biosyn.nih.go.jp/2ndFind/) suggested that four genes *orfA*, *B*, *D*, and *E* adjacent to the *FoFS* (*fusC*) may be involved in the functionalization of fusoxypenes (Fig. 1A and Table S4). *OrfA* encoded a homolog of cytochrome P450 monooxygenase PrhB, which is involved in the biosynthesis of paraherquonin (Matsuda et al. 2016); OrfB is similar to TpcB, a P450 monooxygenase which participates in (-)-terpestacin biosynthesis (Narita et al. 2018); OrfD was assumed to be responsible for C–N hydration, and OrfE was predicted to be a nitrogen assimilation transcription factor (Van Den Berg et al. 2008; Wortman et al. 2009). These proteins are typically involved in primary metabolism processes related to nitrogen fixation in microorganisms and are rarely found in the biosynthetic gene clusters of natural products (Van Den Berg et al. 2008; Wortman et al. 2009; Matsuda et al. 2016; Narita et al. 2018). Further, a detailed analysis of the transmembrane regions of two P450 homologous proteins OrfA and B revealed that the transmembrane region of OrfB is intact and named FusB, whereas that of OrfA is missing, potentially leading to a loss of its catalytic activity when expressed intracellularly (Fig. S1 and Table S5). Given the proximity of these four genes to the *FoFS*, the transformant AO-*orfACD*/*fusBC* harboring *FoFS* and all these four genes were constructed to investigate the metabolites biosynthesized from the *FoFS*-contained gene cluster. The AO harboring the vector plasmid (AO-control) was used as the control.

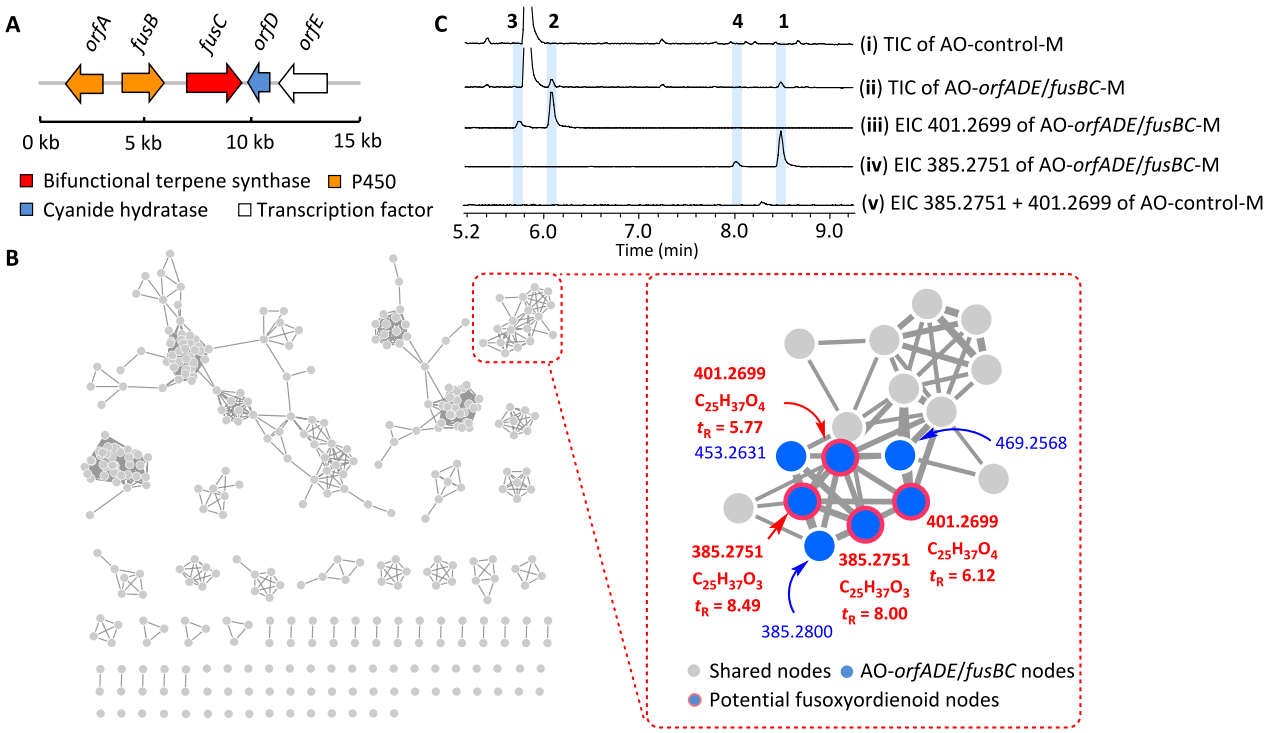

Fig. 1 FBMN-assisted identification of fusoxyordienoids by heterologous expression in *A. oryzae* NSAR1. **A** The gene organization of *fus* gene cluster in *F. oxysporum*. **B** Overview of the molecular networking generated from LC–MS/MS dataset of AO-*orfACD/fusBC* excluding that of AO-control. **C** LC-HRMS analysis of the crude extract from AO-*orfACD/fusBC* and AO small-scale fermentation (marked as M). Only two different products could be observed by comparing the total ion chromatograms (TIC) of crude extract from AO-*orfACD/fusBC* (i) and AO-control (ii). Extracted ion chromatograms (EIC) of crude extract from AO-*orfACD/fusBC* revealed four target products with *m/z* 401.2699 $[M-H]^-$ (iii) and *m/z* 385.2751 $[M-H].^-$ (iv), which were absent in AO-control (v)

FBMN-based discovery of novel fusoxyordienoids A–D (*1–4*)

The transformant AO-*orfACD/fusBC* and the AO-control were separately cultured on 1 g rice medium at 30 °C for 7 days. The fermentation extracts were analyzed by LC-HRMS, and the data were then subjected to Global Natural Products Social (GNPS) analysis. Four clustered nodes with different retention times (t_R) were selected from AO-*orfACD/fusBC* nodes. Their quasi-molecular ion peaks at *m/z* 385.2751 $[M-H]^-$ (calcd for $C_{25}H_{37}O_3$, $t_R = 8.00$ and 8.49 min) and *m/z* 401.2699 $[M-H]^-$ (calcd for $C_{25}H_{37}O_4$, $t_R = 5.77$ and 6.12 min) were observed (Fig. 1B and C).

Further purification and characterization of compounds **1**–**4** (fusoxyordienoids A–D) were carried out through large-scale fermentation (50 kg rice medium) of AO-*orfACD/fusBC* (Fig. 2A). Nuclear magnetic resonance (NMR) spectra showed that all isolated compounds retained the 5/6/7/3/5 ring system as fusoxypene A (**5**) (Fig. 2B) (Jiang et al. 2021a).

Compound **1** was isolated as a colorless crystal, $[\alpha]+7.8$ (*c* 0.09, MeOH). The molecular formula $C_{25}H_{37}O_3$ was deduced by LC-HRMS (found 385.2751 $[M-H]^-$, calcd for 385.2737, Δ 3.6 ppm) (Fig. S2), indicating seven units of unsaturation. The ^{1}H NMR, ^{13}C NMR, and HSQC spectra of **1** revealed the presence of 25 carbon signals, consisting of five methyl singlets, seven methylenes, seven sp^3 methines, a four-substituted olefinic group, three sp^3 quaternary carbons, and one carboxyl moiety. As well, there was a hydroxyl group on the structure of **1** according to its molecular formula. A comparison of the 1D and 2D NMR data of **1** to those of **5** (Jiang et al. 2021a) indicated that they shared the same skeleton except for two substitutions on **1**. The proton and carbon signals of Me-24 and methylene were absent in the ^{1}H and ^{13}C NMR spectra of **1**, while two additional signals assigned for a carboxyl group (δ_C 180.5) and a hydroxyl substitute ($\delta_{C/H}$ 77.3/4.60) were observed. The position of the carboxyl group located at C-24 on the structure of **1** was determined on the basis of the HMBC correlations of H_3-25/C-24, H_3-25/C-19, and H_3-25/C-18 and the $^1H-{}^1H$ COSY correlation of H_3-25/H-19. The hydroxyl group was found to be substituted at C-17 based on the HMBC correlation of H-19/C-17 and $^1H-{}^1H$ COSY correlations of H-16/H-17 and H-17/H-18. Thus, the planar structure of **1** was fully constructed (Fig. 3A, Figs. S3–S7, and Table S6).

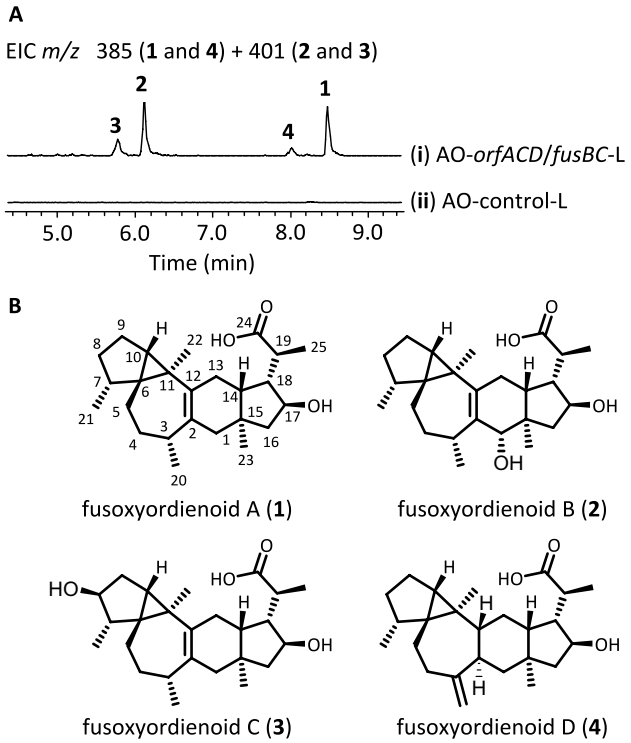

Fig. 2 Large-scale fermentation of AO-*orfACD/fusBC* and the structures of fusoxyordienoids. **A** LC-HRMS profiles of metabolites from large-scale fermentation (marked as L) extracts of AO-*orfACD/fusBC* (i) and AO-control (ii). Chromatograms were extracted at *m/z* 385 and 401 $[M-H]^-$. **B** Structures of and fusoxyordienoids A–D (**1**–**4**)

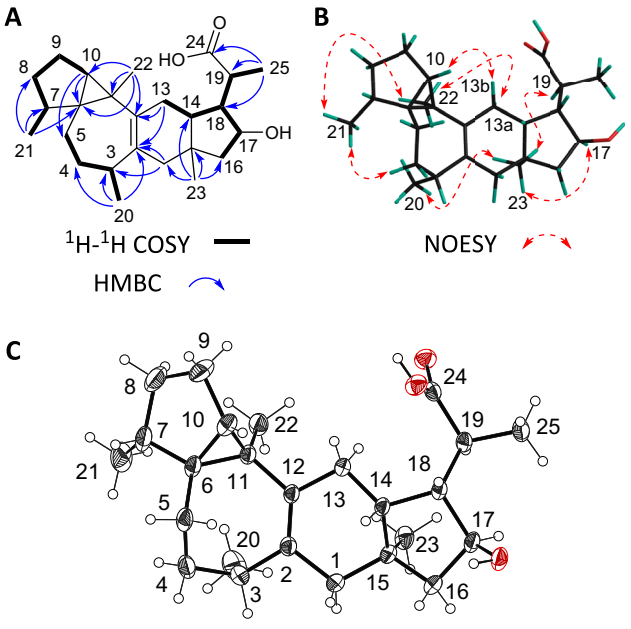

Fig. 3 Determination of the stereochemistry of 1. **A** Key $^1H-^1H$ COSY and HMBC correlations of **1**. **B** Key NOESY correlations of **1**. **C** The ORTEP drawing of the X-ray structure of **1**

Based on key NOESY correlations, including H-10/H-13b, H_3-20/H_3-21, H_3-20/H_3-23, H_3-21/H_3-22, H_3-22/H-13a, and H_3-23/H-17, the relative configuration of **1** could be determined. The orientation of H-17 was therefore deduced to be α (Fig. 3A and Fig. S8). To establish its absolute configuration of compound **1**, a crystal of **1** was obtained using MeOH/EtOAc (4:1 *v*/*v*) at room temperature. The single-crystal X-ray crystallographic experiment was performed using Cu Kα radiation and yielded a Flack parameter of − 0.04(6) (Fig. 3B and Table S7; CCDC 2225788), which secured the absolute configuration of **1** as 3*R*,6*R*,7*R*,10*S*,11*R*,14*R*,15*R*,17*S*,18*R*,19*S*.

Additionally, time-dependent density functional theory (TD-DFT) calculations of the electronic circular dichroism (ECD) spectrum, which were conducted using DFT at the B3LYP/6-31G(d,p) level with the Gaussian 09 program package, further supported the absolute configuration assignment (Figs. S31 and S32). The chemical computation method followed previous research (Jiang et al. 2022a). Comprehensive 1D and 2D NMR experiments allowed for the unambiguous assignment of all signals of compound **1**, which was subsequently named fusoxyordienoid A.

Compound **2** was obtained as a colorless oil, and its molecular formula was determined to be $C_{25}H_{37}O_4$ based on the LC-HRMS at *m/z* 401.2699 ($[M-H]^-$, calcd for 401.2686, Δ 3.1 ppm) (Fig. S9), [α] + 8.0 (*c* 0.05, MeOH). The 1D and 2D NMR spectra of compound **2** closely resembled those of compound **1**, with the difference being the hydroxyl substitution at C-1 of **2**. This substitution was further confirmed by its HMBC correlations of H_3-23/C-1 and H-14/C-1 (Figs. S10–S14 and Table S8). The relative configuration of compound 2 was found to be identical to that of compound **1**, as evidenced by the similar NOESY correlations. The key NOESY signals of H-1/H-3 and H-1/H-14 revealed that the H-1 was in the β-orientation (Fig. S15). Finally, the calculated ECD curve that supported the absolute configuration of **2** was 1*S*,3*R*,6*R*,7*R*,10*S*,11*R*,14*R*,15*R*,17*S*,18*R*,19*S* (Figs. S33 and S34). Thus, the structure of **2** was completely established and named fusoxyordienoid B.

Compound **3**, also isolated as a colorless oil, was assigned a molecular formula of $C_{25}H_{37}O_4$ based on the LC-HRMS experiments (found 401.2699 $[M-H]^-$, calcd for 401.2686, Δ 3.1 ppm) (Fig. S16), [α] + 35.5 (*c* 0.14, MeOH). The 1D and 2D NMR data of **3** were similar to those of **1**. The principal distinguishing feature between these two compounds was the presence of an oxygenated methine group ($\delta_{C/H}$ 80.7/3.94) on **3**. The oxygenated methine group was assigned to C-8 deduced from the HMBC correlation of H_3-21/C-8 and $^1H-^1H$ COSY correlations of H-7/H-8 and H-8/H-9 (Figs. S17–S21 and Table S9). The relative configuration of **3** was determined to be the same as **1** based on the NOESY correlations. And the α-orientation of H-8 was inferred by the key NOESY correlations of H-8/H_3-21

and H-8/H_3-22 (Fig. S22). The absolute configuration of compound **3** was determined to be 3*R*,6*S*,7*S*,8*S*,10*S*,11*R*,14*R*,15*R*,17*S*,18*R*,19*S* by ECD calculation (Figs. S35 and S36), and it was named fusoxyordienoid C.

Compound **4**, isolated as a colorless oil, possessed the molecular formula $C_{25}H_{37}O_3$ according to the LC-HRMS data (found 385.2751 $[M-H]^-$, calcd for 385.2737, Δ 3.6 ppm) (Fig. S23), $[\alpha]-128.5$ (*c* 0.09, MeOH). After a comprehensive analysis of the ^1H and ^{13}C NMR data of **4**, the 1D NMR spectra of **4** were found to exhibit only partial differences from those of compounds **1**–**3** and **5**. Nonetheless, it displayed a structural resemblance to the known compound fusoxypene B, the second product synthesized by FoFS (Jiang et al. 2021a). The distinguishing characteristic of **4** identified from fusoxypene B was the existence of a carboxyl group C-24 (δ_C 180.7), which was deduced by the HMBC correlation of H_3-25/C-24 and H-19 /C-24, and a hydroxyl substitute at C-17 ($\delta_{C/H}$ 76.4/4.63), which was identified by the HMBC correlation of H-19/C-17 and $^1H-^1H$ COSY correlations of H-16/H-17 and H-17/H-18 (Figs. S24–S28 and Table S10). The relative configuration of **4** was found to be identical to that of fusoxypene B based on the comparison of their NOESY correlations. H-17 was assigned to α-orientation according to the crucial NOESY correlations of H_3-23/H-17 (Figure S29). The absolute configuration of **4** was deduced to be 2*R*,6*R*,7*R*,10*R*,11*R*,12*R*,14*R*,15*R*,17*S*,18*R*,19*S* (Figs. S37 and S38) based on its experimental and calculated ECD spectra and was named fusoxyordienoid D.

Characterization of the biosynthetic pathway of fusoxyordienoids A–D (*1–4*)

To illustrate the biosynthetic pathway of **1**–**4**, the metabolites of the four transformants (AO-*fusC*, AO-*orfA*/*fusC*, AO-*fusBC*, and AO-*orfA*/*fusBC*) were analyzed by LC-HRMS experiments. The results showed that the AO-*fusBC* cells could produce these four fusoxyordienoids. Compounds **1**–**4** could also be detected in the AO-*orfA*/*fusBC*, while no products were detected in the AO-*fusC* nor AO-*orfA*/*fusC* cultures (Fig. 4A). Subsequent substrate-feeding experiments were conducted using AO-control and AO-*fusB* strains with fusoxypene A (**5**) as substrate. As expected, all four of these fusoxyordienoids could be detected in the AO-*fusB* transformant but not in the AO-control or non-amended MPY medium (Fig. 4B(i–iii)). Compound **1** was also used as substrate in the subsequent feeding experiment, and **2** and **3** were observed in the AO-*fusB* transformant (Fig. 4B(iv–vi)). A trace compound with *m/z* 401 $[M-H]^-$ could be observed at a t_R of approximately 5.0 min, but it was not related to fusoxyordienoids based on its different MS/MS spectrum. These findings clearly indicated that the putative P450

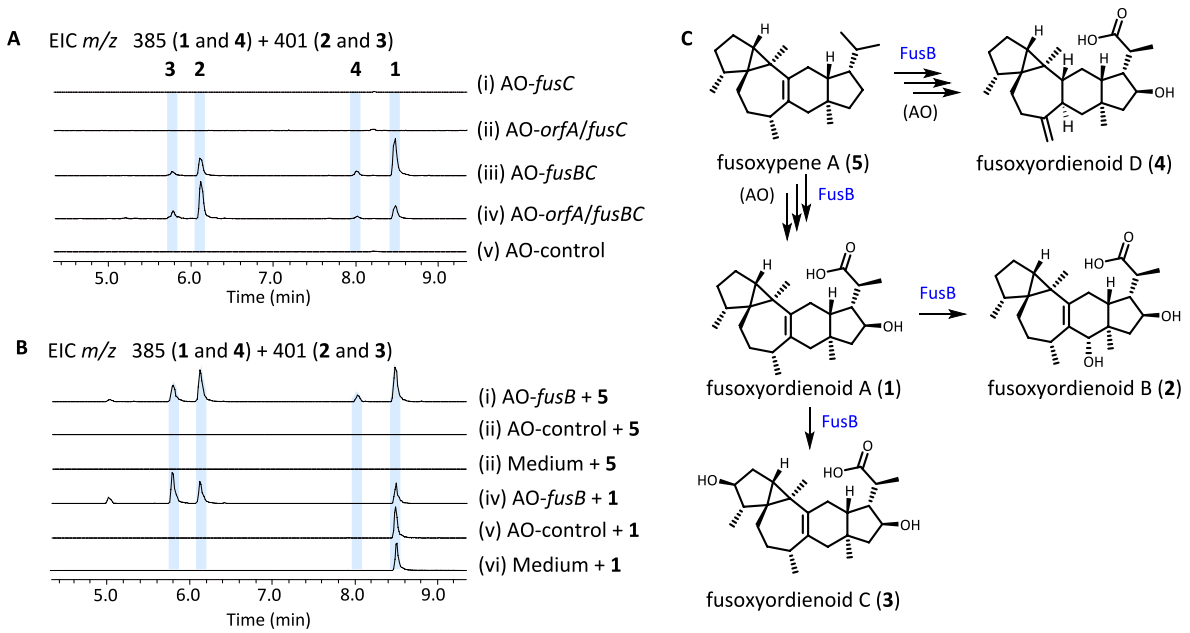

Fig. 4 Elucidated biosynthetic pathway of **1**–**4** by tandem expression and substrate-feeding experiments. **A** LC-HRMS profiles of crude extracts from transformants AO-*fusC* (i), AO-*orfA*/*fusC* (ii), AO-*fusBC* (iii), AO-*orfA*/*fusBC* (iv), and AOcontrol (v), chromatograms were extracted at *m/z* 385+401 $[M-H]^-$. **B** LC-HRMS analysis of AO-*fusB* and AO fed with **5** and **1**. LC-HRMS profiles of fusoxypene A fed to AO-*fusB* (i), AO-control (ii), and non-amended MPY medium (iii) and **1** fed to AO-*fusB* (iv), AO-control (v), and non-amended MPY medium (vi), chromatograms were extracted at *m/z* 401+385 $[M-H]^-$. **C** Proposed fusoxyordienoid biosynthetic pathway in *A. oryzae*

enzyme FusB was responsible for the hydroxylation of fusoxyordienoid A (**1**) at C-1 and C-8. In addition, FusB was involved in the functionalization of C-17 and C-24 on fusoxypene A (**5**).

A putative fusoxyordienoid biosynthetic pathway is depicted in Fig. 4C. Our previous study showed that AtAS, originating from *A. terreus* NIH 2624, could synthesize preaspterpenacid I containing the same pentacyclic ring system as **5**. AtP450 could further introduce a hydroxyl group at C-22 to form preaspterpenacid II (Jiang et al. 2021a). Previously reported aspterpenacid A has an additional oxidation at C-1 compared to preaspterpenacid II (Liu et al. 2016). The oxidation at C-8, C-17, and C-24 in FusB-catalysis revealed the new modifications of the fusoxypene-like pentacycle system.

Biological activity detection of fusoxyordienoids A–D (*1–4*)

All fusoxyordienoids were tested for antimicrobial activity against the pathogenic fungus *Candida albicans* and pathogenic bacteria *E. coli* and *Staphylococcus aureus* using previously described bioassays (Jiang et al. 2021b). However, none of the isolates showed antimicrobial inhibition, all with MIC values > 50 μM. The cytotoxicity of compounds **1** and **4** was also tested by the CCK-8 method (Tominaga et al. 1999; Liu et al. 2011), and both compounds showed moderate effects against A375 human malignant melanoma cells with inhibition rates of 33.01 ± 0.95% and 25.02 ± 0.83%, respectively, at 10 μM (Table 1).

Table 1 Cytotoxicity of compounds **1** and **4**

Cell	Cell inhibition (%)[a] (10 μM)		
	1	**4**	Dox[b]
A549	2.01 ± 1.61	3.22 ± 2.78	70.60 ± 0.83
MKN-45	− 7.67 ± 1.69	10.26 ± 1.82	78.20 ± 1.72
HCT 116	5.90 ± 0.93	5.96 ± 1.21	83.73 ± 1.67
HeLa	4.76 ± 0.75	6.31 ± 0.37	90.60 ± 0.25
K-562	5.13 ± 1.66	6.22 ± 3.95	84.55 ± 0.24
786-O	1.85 ± 3.21	5.53 ± 3.20	87.55 ± 1.40
TE-1	7.73 ± 3.25	2.23 ± 1.49	81.31 ± 0.56
5637	− 0.80 ± 0.98	− 0.76 ± 0.54	93.57 ± 0.54
GBC-SD	2.73 ± 2.13	1.53 ± 3.48	81.62 ± 0.66
L-02	4.74 ± 2.17	3.37 ± 1.75	91.42 ± 0.89
MCF7	7.19 ± 0.58	11.57 ± 1.81	47.17 ± 0.96
HepG2	5.56 ± 3.87	6.64 ± 2.98	72.45 ± 0.56
SF126	1.48 ± 0.73	0.78 ± 0.80	68.98 ± 1.15
DU145	− 1.78 ± 3.26	0.70 ± 0.63	66.52 ± 1.33
CAL-62	1.33 ± 2.20	− 0.06 ± 3.34	73.19 ± 0.55
PATU8988T	11.17 ± 1.56	7.22 ± 0.99	86.62 ± 0.34
HOS	4.49 ± 2.69	10.93 ± 2.68	85.73 ± 0.11
A-375	33.01 ± 0.95	25.02 ± 0.83	77.07 ± 0.74
A-673	− 6.27 ± 1.55	0.00 ± 1.22	71.63 ± 1.19
293 T	18.40 ± 1.24	4.06 ± 1.92	88.78 ± 0.74

[a]Cell inhibition rates are the mean ± SD of three independent experiments at a corresponding concentration

[b]Positive control: doxorubicin hydrochloride

Discussion

Terpenoids are one of the most extensive family of compounds (Kumari et al. 2013; Quin et al. 2014). Sesterterpenoids comprise a mere 2% of terpenoids and are known for their diverse polycyclic scaffolds and various bioactivity, including anti-cancer, anti-inflammatory, anti-malarial, and anti-tuberculosis, making them invaluable for pharmaceutical innovation (Jiang et al. 2021b; Li and Gustafson 2021). Representative active sesterterpenoids include ophiobolin A, renowned for its anti-tumor efficacy, and terpestacin, recognized for its ability to impede the formation of syncytia associated with HIV infection (Leung et al. 1985; Chiba et al. 2013; Narita et al. 2017). The fusoxyordienoids identified in this study also showed some inhibitory effects on tumor cells, further reinforcing the significance of sesterterpenoids as an important source of bioactive compounds and providing candidates for the development of anti-cancer drugs.

Cytochrome P450 monooxygenase is one of the most important terpenoid tailoring enzymes (Zhang and Li 2017; Li et al. 2020; Zhang et al. 2021). Unlike specific reaction-modifying enzymes (such as glycosyltransferase, phosphatase, and methyltransferase), P450 catalyzes the oxidation of terpene-inert C–H bonds and exhibits a wide range of catalytic reactions, including hydroxylation, epoxidation, and carbon–carbon bond breaking (Zhang and Li 2017). This allows for the production of structurally diverse terpenoids through a "mini gene cluster" that only contains a terpene synthase and P450. One latest example is the sesquiterpenoid BGC *bip*, which consists of only one sesquiterpene synthase and one P450 enzyme but generates four seco-sativenes (Zhang et al. 2024a, 2024b). Due to the marked flexibility in their active site region, P450s frequently exhibit multifunctional catalytic capabilities in the biosynthesis of natural products (V. Espinoza et al. 2021; Ashworth et al. 2022). Similar findings were observed in our study, which isolated and identified four sesterterpenoids with different structures and functions by heterologous characterization of the "mini gene cluster" *fus*. The P450 FusB in our study could catalyze hydroxylation at two distinct sites on **1**, potentially due to the presence of two different binding conformations of **1** within the pocket. This hypothesis requires further elucidation of the catalytic mechanism of FusB through methods such as molecular docking. All these indicate that P450 plays a

key role in shaping the structure and functional diversity of terpenoids and also suggest that mining terpenoid P450s may provide a new perspective for the discovery of novel terpenoids.

FBMN, a type of MN, interconnects secondary metabolites to provide a visual approach for natural product discovery (Han et al. 2022; Afoullouss et al. 2022; Wang et al., 2024). Our group has previously utilized classical MN to identify new natural products from wild-type strains (Zhu et al. 2020). Based on prior experience, this study combines the advantages of FBMN with heterologous expression, simplifying the preliminary analysis process of heterologous expression, saving time and costs, and preventing the oversight of low-yield secondary metabolites in crude extracts. Our approach enables the discovery of trace differential products from micro-fermentation.

In summary, we identified the biosynthetic gene cluster for the novel sesterterpene skeleton fusoxypene A based on our previous study, and four new products, fusoxyordienoids, derived from the oxidation of fusoxypene A at different sites, were characterized here through a FBMN-based heterologous expression strategy. Further preliminary biosynthetic pathway analyses indicated that a putative P450 FusB was involved in the oxidation of fusoxypene A. This work provides a valuable strategy for the efficient discovery of novel natural products and tailoring genes through visualizing the trace products via heterologous expression and lays the groundwork for future discoveries.

Acknowledgements We would like to express our sincere gratitude for the financial support received from various sources.

Author contribution XL and LJ: project design, consortium supervision, and writing revision. TH: genomic data resources and writing Revision. KL and DY: investigation, experiment execution, and formal analysis. XL, XW, CX, KL, GZ, and SL: investigation and result validation. LZ: writing revision.

Funding This work was supported by the National Natural Science Foundation of China (21977029, 21907031) to XL and LJ and the National Key Research and Development Program of China (2019YFA0906200 and 2020YFA090032) to XL and LZ. We are grateful for the funding support from The Science and Technology Commission of Shanghai Municipality (21NL2600100) to XL. Furthermore, we would like to acknowledge the Natural Science and Engineering Research Council of Canada for funding the genome sequencing and assembly of *F. oxysporum* strain FO14005 by TH.

Data availability All data generated or analyzed during this study are included in the published article and electrical supplementary material available at https://doi.org/10.1007/s00253-024-13299-9.

Declarations

Ethical statement This article does not contain any studies with human participants or animals performed by any of the authors.

Conflict of interest The authors declare no competing interest.

References

Afoullouss S, Balsam A, Allcock AL, Thomas OP (2022) Optimization of LC-MS2 data acquisition parameters for molecular networking applied to marine natural products. Metabolites 12(3):245. https://doi.org/10.3390/metabo12030245

Ashworth MA, Bombino E, de Jong RM, Wijma HJ, Janssen DB, McLean KJ, Munro AW (2022) Computation-aided engineering of cytochrome P450 for the production of pravastatin. ACS Catal 12(24):15028–15044. https://doi.org/10.1021/acscatal.2c03974

Chambers MC, Maclean B, Burke R, Amodei D, Ruderman DL, Neumann S, Gatto L, Fischer B, Pratt B, Egertson J (2012) A cross-platform toolkit for mass spectrometry and proteomics. Nat Biotechnol 30(10):918–920. https://doi.org/10.1038/nbt.2377

Chiba R, Minami A, Gomi K, Oikawa H (2013) Identification of ophiobolin F synthase by a genome mining approach: a sesterterpene synthase from *Aspergillus clavatus*. Org Lett 15(3):594–597. https://doi.org/10.1021/ol303408a

Gong D-Y, Chen X-Y, Guo S-X, Wang B-C, Li B (2021) Recent advances and new insights in biosynthesis of dendrobine and sesquiterpenes. Appl Microbiol Biotechnol 105(18):6597–6606. https://doi.org/10.1007/s00253-021-11534-1

Guo J, Cai Y-S, Cheng F, Yang C, Zhang W, Yu W, Yan J, Deng Z, Hong K (2021) Genome mining reveals a multiproduct sesterterpenoid biosynthetic gene cluster in *Aspergillus ustus*. Org Lett 23(5):1525–1529. https://doi.org/10.1021/acs.orglett.0c03996

Han J, Chen B, Zhang R, Zhang J, Dai H, Wang T, Sun J, Zhu G, Li W, Li E (2022) Exploring verrucosidin derivatives with glucose-uptake-stimulatory activity from *Penicillium cellarum* using MS/MS-based molecular networking. J Fungi 8(2):143. https://doi.org/10.3390/jof8020143

Jiang L, Zhang X, Sato Y, Zhu G, Minami A, Zhang W, Ozaki T, Zhu B, Wang Z, Wang X, Lv K, Zhang J, Wang Y, Gao S, Liu C, Tom H, Zhang L, Oikawa H, Liu X (2021a) Genome-based discovery of enantiomeric pentacyclic sesterterpenes catalyzed by fungal bifunctional terpene synthases. Org Lett 23(12):4645–4650. https://doi.org/10.1021/acs.orglett.1c01361

Jiang L, Zhu G, Han J, Hou C, Zhang X, Wang Z, Yuan W, Lv K, Cong Z, Wang X, Chen X, Karthik L, Yang H, Wang X, Tan G, Liu G, Zhao L, Xia X, Liu X, Gao S, Ma L, Liu M, Ren B, Dai H, Quinn RJ, Tom H, Zhang J, Zhang L, Liu X (2021b) Genome-guided investigation of anti-inflammatory sesterterpenoids with 5–15 trans-fused ring system from phytopathogenic fungi. Appl Microbiol Biotechnol 105(13):5407–5417. https://doi.org/10.1007/s00253-021-11192-3

Jiang L, Lv K, Zhu G, Lin Z, Zhang X, Xing C, Yang H, Zhang W, Wang Z, Liu C, Qu X, Hsiang T, Zhang L, Liu X (2022a) Norditerpenoids biosynthesized by variediene synthase-associated P450 machinery along with modifications by the host cell *Aspergillus oryzae*. Synth Syst Biotechnol 7(4):1142–1147. https://doi.org/10.1016/j.synbio.2022.08.002

Jiang L, Yang H, Zhang X, Li X, Lv K, Zhang W, Zhu G, Liu C, Wang Y, Hsiang T, Zhang L, Liu X (2022b) Schultriene and nigtetraene: two sesterterpenes characterized from pathogenetic fungi via genome mining approach. Appl Microbiol Biotechnol 106(18):6047–6057. https://doi.org/10.1007/s00253-022-12125-4

Jin FJ, Maruyama J-i, Juvvadi PR, Arioka M, Kitamoto K (2004) Development of a novel quadruple auxotrophic host transformation system by *argB* gene disruption using *adeA* gene and exploiting adenine auxotrophy in *Aspergillus oryzae*. FEMS Microbiol Lett 239(1):79–85. https://doi.org/10.1016/j.femsle.2004.08.025

Keller NP (2019) Fungal secondary metabolism: regulation, function and drug discovery. Nat Rev Microbiol 17(3):167–180. https://doi.org/10.1038/s41579-018-0121-1

Kumari S, Priya P, Misra G, Yadav G (2013) Structural and biochemical perspectives in plant isoprenoid biosynthesis. Phytochem Rev 12(2):255–291. https://doi.org/10.1007/s11101-013-9284-6

Leung PC, Taylor WA, Wang JH, Tipton CL (1985) Role of calmodulin inhibition in the mode of action of ophiobolin A. Plant Physiol 77(2):303–308. https://doi.org/10.1104/pp.77.2.303

Li K, Gustafson KR (2021) Sesterterpenoids: chemistry, biology, and biosynthesis. Nat Prod Rep 38(7):1251–1281. https://doi.org/10.1039/d0np00070a

Li Z, Jiang Y, Guengerich FP, Ma L, Li S, Zhang W (2020) Engineering cytochrome P450 enzyme systems for biomedical and biotechnological applications. J Biol Chem 295(3):833–849. https://doi.org/10.1074/jbc.REV119.008758

Liu X, Wei W, Wang C, Yue H, Ma D, Zhu C, Ma G, Du Y (2011) Apoferritin-camouflaged Pt nanoparticles: surface effects on cellular uptake and cytotoxicity. J Mater Chem 21(20):7105–7110. https://doi.org/10.1039/C1JM10575B

Liu Z, Chen Y, Chen S, Liu Y, Lu Y, Chen D, Lin Y, Huang X, She Z (2016) Aspterpenacids A and B, two sesterterpenoids from a mangrove endophytic fungus *Aspergillus terreus* H010. Org Lett 18(6):1406–1409. https://doi.org/10.1021/acs.orglett.6b00336

Matsuda Y, Iwabuchi T, Fujimoto T, Awakawa T, Nakashima Y, Mori T, Zhang H, Hayashi F, Abe I (2016) Discovery of key dioxygenases that diverged the paraherquonin and acetoxydehydroaustin pathways in *Penicillium brasilianum*. J Am Chem Soc 138(38):12671–12677. https://doi.org/10.1021/jacs.6b08424

Minami A, Ozaki T, Liu C, Oikawa H (2018) Cyclopentane-forming di/sesterterpene synthases: widely distributed enzymes in bacteria, fungi, and plants. Nat Prod Rep 35(12):1330–1346. https://doi.org/10.1039/c8np00026c

Mitsuhashi T, Abe I (2018) Chimeric terpene synthases possessing both terpene cyclization and prenyltransfer activities. ChemBioChem 19(11):1106–1114. https://doi.org/10.1002/cbic.201800120

Narita K, Chiba R, Minami A, Kodama M, Fujii I, Gomi K, Oikawa H (2016) Multiple oxidative modifications in the ophiobolin biosynthesis: P450 oxidations found in genome mining. Org Lett 18(9):1980–1983. https://doi.org/10.1021/acs.orglett.6b00552

Narita K, Sato H, Minami A, Kudo K, Gao L, Liu C, Ozaki T, Kodama M, Lei X, Taniguchi T (2017) Focused genome mining of structurally related sesterterpenes: enzymatic formation of enantiomeric and diastereomeric products. Org Lett 19(24):6696–6699. https://doi.org/10.1021/acs.orglett.7b03418

Narita K, Minami A, Ozaki T, Liu C, Kodama M, Oikawa H (2018) Total biosynthesis of antiangiogenic agent (−)-terpestacin by artificial reconstitution of the biosynthetic machinery in *Aspergillus oryzae*. J Org Chem 83(13):7042–7048. https://doi.org/10.1021/acs.joc.7b03220

Nothias L-F, Petras D, Schmid R, Dührkop K, Rainer J, Sarvepalli A, Protsyuk I, Ernst M, Tsugawa H, Fleischauer M (2020) Feature-based molecular networking in the GNPS analysis environment. Nat Methods 17(9):905–908. https://doi.org/10.1038/s41592-020-0933-6

Oikawa H (2020) Reconstitution of biosynthetic machinery of fungal natural products in heterologous hosts. Biosci Biotechnol, Biochem 84(3):433–444. https://doi.org/10.1080/09168451.2019.1690976

Pluskal T, Castillo S, Villar-Briones A, Orešič M (2010) MZmine 2: modular framework for processing, visualizing, and analyzing mass spectrometry-based molecular profile data. BMC Bioinformatics 11(1):1–11. https://doi.org/10.1186/1471-2105-11-395

Pye CR, Bertin MJ, Lokey RS, Gerwick WH, Linington RG (2017) Retrospective analysis of natural products provides insights for future discovery trends. Proc Natl Acad Sci U S A 114(22):5601–5606. https://doi.org/10.1073/pnas.1614680114

Quin MB, Flynn CM, Schmidt-Dannert C (2014) Traversing the fungal terpenome. Nat Prod Rep 31(10):1449–1473. https://doi.org/10.1039/c4np00075g

Ro D-K, Paradise EM, Ouellet M, Fisher KJ, Newman KL, Ndungu JM, Ho KA, Eachus RA, Ham TS, Kirby J (2006) Production of the antimalarial drug precursor artemisinic acid in engineered yeast. Nature 440(7086):940–943. https://www.nature.com/articles/nature04640

Standards NCfCL (1997) Reference method for broth dilution antifungal susceptibility testing of yeasts: tentative standard. NCCLS Document M27-A

Tominaga H, Ishiyama M, Ohseto F, Sasamoto K, Hamamoto T, Suzuki K, Watanabe M (1999) A water-soluble tetrazolium salt useful for colorimetric cell viability assay. Anal Commun 36(2):47–50. https://doi.org/10.1039/A809656B

Toyomasu T, Tsukahara M, Kaneko A, Niida R, Mitsuhashi W, Dairi T, Kato N, Sassa T (2007) Fusicoccins are biosynthesized by an unusual chimera diterpene synthase in fungi. Proc Natl Acad Sci U S A 104(9):3084–3088. https://doi.org/10.1073/pnas.0608426104

Van Den Berg MA, Albang R, Albermann K, Badger JH, Daran J-M, Driessen M, AJ, Garcia-Estrada C, Fedorova ND, Harris DM, Heijne WH (2008) Genome sequencing and analysis of the filamentous fungus *Penicillium chrysogenum*. Nat Biotechnol 26(10):1161–1168. https://doi.org/10.1038/nbt.1498

V. Espinoza R, Haatveit KC, Grossman SW, Tan JY, McGlade CA, Khatri Y, Newmister SA, Schmidt JJ, Garcia-Borràs M, Montgomery J (2021) Engineering P450 TamI as an iterative biocatalyst for selective late-stage C-H functionalization and epoxidation of tirandamycin antibiotics. ACS Catal 11(13):8304–8316. https://doi.org/10.1021/acscatal.1c01460

Wang M, Carver JJ, Phelan VV, Sanchez LM, Garg N, Peng Y, Nguyen DD, Watrous J, Kapono CA, Luzzatto-Knaan T (2016) Sharing and community curation of mass spectrometry data with Global Natural Products Social Molecular Networking. Nat Biotechnol 34(8):828–837. https://doi.org/10.1038/nbt.3597

Watrous J, Roach P, Alexandrov T, Heath BS, Yang JY, Kersten RD, van der Voort M, Pogliano K, Gross H, Raaijmakers JM (2012) Mass spectral molecular networking of living microbial colonies. Proc Natl Acad Sci U S A 109(26):E1743–E1752. https://doi.org/10.1073/pnas.1203689109

Wortman JR, Gilsenan JM, Joardar V, Deegan J, Clutterbuck J, Andersen MR, Archer D, Bencina M, Braus G, Coutinho P (2009) The 2008 update of the *Aspergillus nidulans* genome annotation: a community effort. Fungal Genet Biol 46(1):S2–S13. https://doi.org/10.1016/j.fgb.2008.12.003

Zhang C, Hong K (2020) Production of terpenoids by synthetic biology approaches. Front Bioeng Biotechnol 8:347. https://doi.org/10.3389/fbioe.2020.00347

Zhang X, Li S (2017) Expansion of chemical space for natural products by uncommon P450 reactions. Nat Prod Rep 34(9):1061–1089. https://doi.org/10.1039/c7np00028f

Zhang X, Guo J, Cheng F, Li S (2021) Cytochrome P450 enzymes in fungal natural product biosynthesis. Nat Prod Rep 38(6):1072–1099. https://doi.org/10.1039/d1np00004g

Zhang H, Zhao H, Huang Y, Zou Y (2024a) Genome mining reveals the biosynthesis of sativene and its oxidative conversion to seco-sativene. Org Lett 26(1):338–343. https://doi.org/10.1021/acs.orglett.3c04005

Zhang MM, Long Y, Li Y, Cui JJ, Lv T, Luo S, Gao K, Dong SH (2024b) Divergent biosynthesis of bridged polycyclic sesquiterpenoids by a minimal fungal biosynthetic gene cluster. J Nat Prod 87(4):893–905. https://doi.org/10.1021/acs.jnatprod.3c01161

Zhu G, Hou C, Yuan W, Wang Z, Zhang J, Jiang L, Karthik L, Li B, Ren B, Lv K, Lu W, Cong Z, Dai H, Tom H, Zhang L, Liu X (2020) Molecular networking assisted discovery and biosynthesis elucidation of the antimicrobial spiroketals epicospirocins. Chem Commun 56(70):10171–10174. https://doi.org/10.1039/D0CC03990J